14th European Signal Processing Conference (EUSIPCO 2006), Florence, Italy, September 4-8, 2006, copyright by EURASIP

GABOR FEATURE VECTORS TO DETECT CHANGES AMONGST TIME SERIES: A GEOACOUSTIC EXAMPLE

Patrick Oonincx[1], *Anthony Auger-Ottavi*[2], *Louis le Proux de la Riviere*[2], *Jean-Pierre Hermand*[1]

[1] Netherlands Defense Academy
P.O. Box 10000, 1780 CA Den Helder, The Netherlands
phone: + 31233657134, fax: + 31223657414,
email: p.j.oonincx@kim.nl

[2] Ecole Navale
B.P. 600, F-29240 Brest Naval, France
phone: + 33298233837, fax: +33298233857

ABSTRACT

We use the Matching Pursuit algorithm to decompose Green's functions of varying systems. Feature vectors representing the Green's functions are constructed from the pursuit approximation. Increasing distances among these vectors are related to changing parameters in the systems. The quality of the entries of the feature vectors is discussed and the distances between these vectors are measured following an adaptive approach. Results of the method are illustrated using a geophysical example.

1. INTRODUCTION

We consider systems $\mathscr{L}(x)$, depending on one or more parameters x, whose corresponding impulse responses/Green's functions g_x also depend in a more or less continuous way on x. One can think of x as a location or environmental variable, like temperature that can influence impendances in an electric circuit. Changing values for x will effect the impulse responses g_x and so, by comparing different g_x one is also able to detect changes in the system $\mathscr{L}(x)$, and therefore in the parameter x.

A way to analyse changing impulse responses is by correlating the various g_x with each other. A high degree of correlation can be related to slight changes in the parameter(s) x, while a very low correlation rate may indicate abrupt changes/singularities in x.

To compute a correlation rate between different g_x several commonly used statistical measures are available. However, these classical measures become less effective if g_x consists of combined characteristic wave packets all representing a typical physical feature of the problem given by $\mathscr{L}(x)$. All these wave packets may be influenced in different manners by changing x. In such cases one should first identify typical waveguides appearing in each g_x and then compare these waveguides in the changing setting.

A signal decomposition scheme that fits the requirements mentioned above is the Matching Pursuit algorithm [1]. This method is able to decompose physical data into wave packets that match best with the original waveguides in g_x. Furthermore, the decomposition is sparse and all wave packets, called atoms, are well localised in time, scale and frequency.

In an earlier paper [2] we already discussed the use of Matching Pursuit in a geoacoustic setting. In a shallow water environment from a fixed location sonar pings were transmitted towards a receiver coupled to a drifting buoy. Acoustic impulse responses were measured at the receiver as it drifts away from the source passing different sedimental regions. Because of scattering with changing bottom properties along the buoy track the measured impulse responses along the track are also effected. They can be regarded as an example of Green's function $g_x(t)$, signals that strongly depend on the position of measurement x. Preliminary results were achieved for identifying changes in sea bottom properties, i.e., changing sediments.

In this paper we present a more sophisticated approach, that not only yields better results for the geoacoustic example, but also offers opportunities to analyse a larger class of problems in different types of physical settings, but all dealing with changing system variables x in a system $\mathscr{L}(x)$. We recall the Matching Pursuit algorithm in Section 2. In Section 3 we describe how the wave packets appearing in the MP decomposition of changing g_x can be compared in an efficient way. For this we discuss the topic of feature vectors. Section 4 discusses several ways of optimising the use of feature vectors for these type of problems, and for the geoacoustic example in particular. Finally, Section 5 shows the effect of our new approach reconsidering the geoacoustic example.

2. THE MATCHING PURSUIT APPROACH

We recall the Matching Pursuit (MP) signal decomposition algorithm given by Mallat and Zhang [1]. This method projects a signal $s \in L^2(\mathbb{R})$ on a redundant set of monofrequent scaled waves $h_\gamma \in L^2(\mathbb{R})$, called atoms, that result from scaling, frequency modulation and time shifting of one given window function h, i.e.,

$$h_\gamma(u) = \frac{1}{\sqrt{a}} h\left(\frac{u-t}{a}\right) e^{-juf}, \ \gamma = (a,t,f) \in \mathbb{R}^+ \times \mathbb{R}^2. \quad (1)$$

We suppose h to be normalized in energy ($\|h\|_2 = 1$). Here, we consider Gabor atoms h_γ, given by $h(u) = 2^{1/4} e^{-\pi t^2}$, i.e., the Gaussian window function with width $1/2\pi$.

The algorithm starts by choosing a (redundant) countable set of atoms h_{γ_n}, that is complete in $L^2(\mathbb{R})$. This can be achieved by means of a tiling in the time-scale-frequency domain (t,a,f). Once this dictionary of atoms is available, optimization of a cost function is used to find an atom, say h_{γ_0}, that matches best with the signal s by means of the L^2-inner product, i.e.,

$$| < s, h_{\gamma_0} > | \geq | < s, h_{\gamma_n} > |, \ n > 0. \quad (2)$$

The signal s is then decomposed into

$$s = < s, h_{\gamma_0} > h_{\gamma_0} + R_1 s, \quad (3)$$

with $R_1 s$ a residual. In a rather straightforward way we deduce $< R_1 s, h_{\gamma_0} > = 0$ and therefore

$$\|s\|^2 = | < s, h_{\gamma_0} > |^2 + \|R_1 s\|^2. \quad (4)$$

Next, $R_1 s$ is decomposed in a similar way, namely by finding the best matching atom h_{γ_1}, i.e.,

$$| < R_1 s, h_{\gamma_1} > | \geq | < R_1 s, h_{\gamma_n} > |, \; n > 1.$$

This yields

$$R_1 s = < R_1 s, h_{\gamma_1} > h_{\gamma_1} + R_2 s,$$

and in an analogous way

$$\|R_1 s\|^2 = | < s, h_{\gamma_1} > |^2 + \|R_2 s\|^2.$$

By iteration we end up with the atomic decomposition

$$s = \sum_{n=0}^{\infty} < R_n s, h_{\gamma_n} > h_{\gamma_n}, \tag{5}$$

with $R_0 s = s$ by definition. Furthermore, we have

$$\|s\|^2 = \sum_{n=0}^{\infty} | < R_n s, h_{\gamma_n} > |^2. \tag{6}$$

Convergence of the projection pursuit algorithms was conjectured by P. Huber [3] and later proved by L. Jones [4]. The MP algorithm establishes a nonlinear decomposition of a signal s into a sum of atoms with some desirable physical signature. Moreover, although the decomposition is nonlinear we maintain an energy conservation law as if it was a linear orthogonal decomposition. Equation (6) can be useful for measuring the quality of an approximation of a signal s using a decomposition with only N atoms. The ratio

$$E_s(N) = \frac{\sum_{n=0}^{N-1} | < R_n s, h_{\gamma_n} > |^2}{\|s\|^2} \tag{7}$$

measures the amount of energy from the original signal represented by an N-atom decomposition. Observe that the L^2-approximation error is given by

$$\|s - s_N\|^2 = \sum_{n=N}^{\infty} | < R_n s, h_{\gamma_n} > |^2 = \|s\|^2 (1 - E_s(N)),$$

with s_N the approximation of s using the first N atoms. Straightforwardly, we have from (6)

- $0 \leq E_s(N) \leq 1$,
- $\lim_{N \to \infty} E_s(N) = 1$,
- $E_s(N) < E_s(N+1)$.

Furthermore, since the Pursuit algorithm chooses at each iteration step the most matching atom, $E_s(N)$ will be a concave function. Therefore, summing $| < R_n s, h_{\gamma_n} > |^2$ at each iteration n in the MP algorithm yields a stop criterion to finish the iterative process once a desired degree of approximation has been reached. Experiments with different types of physical data have shown that typically $E_s(N) \sim 0.75$ for only a small number N, e.g., $N \sim 5$. In Section 4 we discuss the values of the energy ratio in more detail for the geoacoustic example, as introduced in Section 1.

3. THE CONCEPT OF GABOR FEATURE VECTORS

A common approach to measure similarities between images is to use feature vectors. These are vectors associated to an image as a kind of representative of that image. For a set of more or less related images a set of associated feature vectors can be constructed. The entries of such vectors represent typical features for the images, e.g. colour, symmetry measures, affine invariances of the objects in the image.

Measuring distances between the feature vectors yields information on the degree of similarity between images in a given set. For a proper analysis of the similarities the features should be strongly discriminating, i.e., differences in one entry of the vector should be associated with 'visible differences' in the corresponding images. Furthermore, since feature vectors represent objects with many data entries (like an image of 256×256 pixels) by a relatively low dimensional vector, one should take care that mapping objects onto a feature vector is bijective within a given class of objects.

In this paper we identify (geophysical) signals $s_i \in L^2(\mathbb{R})$ with feature vectors $\vec{v}_i$ using (5). Moreover, we represent signals s_i by $4N$-dimensional feature vectors $\vec{v}_i$, given by

$$\vec{v}_i = (c_{i,1}, a_{i,1}, f_{i,1}, t_{i,1}, \cdots, c_{i,N}, a_{i,N}, f_{i,N}, t_{i,N}), \tag{8}$$

the collection of all MP parameters of $s_{i,N}$, the N-term Gabor decomposition of s_i, with $c_{i,k} := < R_{k-1} s_i, h_{\gamma_{k-1}} >$. Since waveforms appearing in geophysical data are very similar to the functions in the dictionary of Gabor atoms, every group of four related entries in $\vec{v}_i$ is able to represent one physical characteristic of the given signal. This property makes such a Gabor feature vector $\vec{v}_i$ a useful tool for discriminating different physical signals. Convergence result (5) also guarantees a bijective mapping from s_i to $\vec{v}_i$, which makes the vectors well-defined.

The dimension $4N$ of the feature vectors is determined by the number of atoms (N) used for approximating all s_i. This number will be related to the approximation error

$$\|s_i\|^2 (1 - E_{s_i}(N)).$$

For all s_i a number N_i is determined, such that the approximation error is less than $\delta \cdot \|s_i\|^2$, for a given $\delta > 0$. Since distances between vectors can only be measured if the vectors have the same dimension we have to fix N for all s_i. The number of atoms considered for all s_i will be the maximum of all N_i.

An alternative approach is to construct for each s_i an N_i-dimensional feature vector $\vec{v}_i$. The distance between two vectors $\vec{v}_i$ and $\vec{v}_j$ can be measured by considering $\vec{v}_i$ and $\vec{v}_j$ restricted to the first $4 \cdot \max(N_i, N_j)$ entries. The advantage of such an adaptive approach is that the distances are truely measuring coherent structures within the main part of the signals. The first few atoms will be related to the most dominant physical structures in the signals. Atoms with higher index numbers will also be related to artefacts (noisy components) within a signal s_i. These can be covered by atoms with index numbers between N_i and N, the maximum of all N_i, if this maximum differs too much from N_i. The undesirable influence of these signal parts can be diminished in the calculations following the adaptive approach. Experiments for choosing a suitable number of atoms N_i, i.e., an appropriate approximation error δ, is discussed in the next section.

Both for the adaptive and the non-adaptive approach mutual distances between feature vectors are measured using the weighted Euclidean distance [6]

$$d_\sigma(\vec{v}_i,\vec{v}_j) = \|\mathrm{diag}\,(\sigma_1,\cdots,\sigma_{4N})^{-1}\,(\vec{v}_i-\vec{v}_j)\|, \qquad (9)$$

with $\|\cdot\|$ the usual Euclidean vector norm and with σ_l the variance of the set $\{\,\vec{v}_i(l)\,\}$, for $l = 1,\ldots,4N$. Observe, that in the adaptive approach we take $N = 4\cdot\max(N_i,N_j)$.

4. GABOR FEATURE VECTORS IN PRACTICE

For comparing typical waveforms appearing in related signals s_i one can use the Gabor Feature Vector approach as described in the previous section. For particular problems the approach can be further optimised as some of the parameters may be of greater importance for the discriminating character of the vectors than other physical variables. Also the number of atoms N taken into account can be optimised for a given problem. Although it seems that these optimisations are strictly problem related, we can also make some modifications for a general problem setting. Both classes of modifications are discussed in this section

4.1 General Modifications

Weighted distance measures already take the diversity in ranges of the parameters into account to get balanced feature vectors. However, if a feature vector entry does not have a substantial contribution to the discriminating and identifying character of the vectors, one better omits the entry for distance calculations. Typically this is the case for position parameters $t_{i,n}$ once all s_i are centered around $t_{i,0}$. Note that one should be aware whether waveforms, to be compared amonst s_i, appear at similar places within the given set of data. Data related to one physical phenomenon/mathematical model often will satisfy this criterion for a large amount of most important $t_{i,n}$. Particularly, for our geoacoustic example experiments showed that normalised position parameters in the MP decomposition have negligable influence on the distance computations.

An other a-priori optimisation step when comparing characteristics of waveforms is given by a normalisation of all s_i in L^2-norm, such that all s_i have energy equal to 1. This normalisation is given by

$$\tilde{s_i} = \frac{s_i}{\|s_i\|}.$$

Of course the energy in each s_i can be an important feature as well. Therefore $\|s_i\|^2$ is added to each feature vector $\vec{v}_i$ as an additional entry. For the geoacoustic example this type of normalisation means a great improvement of the results. This is due to the fact that when i becomes larger the length of the propagation path from source to receiver becomes larger as well, yielding a kind of linear decrease of the signal's amplitude. We expect that this type of normalisation can have similar impact on the results obtained for other kinds of physical problems.

A last general improvement concerns the interpretation of distances between feature vectors. In practice the outcome of the distance calculations may be influenced effected by environmental artefacts ('noise'). If changes in s_i depend continuously on i, one will be interested in values of $d\,f_i = d_\sigma(\vec{v}_i,\vec{v}_{i-1})$ compared to $d\,f_{i-1}, d\,f_{i-2},\ldots$ and $d\,f_{i+1}, d\,f_{i+2},\ldots$. A changing situation in the system will always be noticed by more than one distance as given above. Therefore we suggest the following measure to indicate changing feature vectors locally around sample i:

$$\mathrm{mean}\begin{pmatrix} d_\sigma(\vec{v}_i,\vec{v}_{i+1}) & d_\sigma(\vec{v}_{i-1},\vec{v}_{i+1}) & d_\sigma(\vec{v}_{i-2},\vec{v}_{i+1}) \\ d_\sigma(\vec{v}_i,\vec{v}_{i+2}) & d_\sigma(\vec{v}_{i-1},\vec{v}_{i+2}) & d_\sigma(\vec{v}_{i-2},\vec{v}_{i+2}) \\ d_\sigma(\vec{v}_i,\vec{v}_{i+3}) & d_\sigma(\vec{v}_{i-1},\vec{v}_{i+3}) & d_\sigma(\vec{v}_{i-2},\vec{v}_{i+3}) \end{pmatrix}.$$

We will denote this measure, the mean of all 9 distances around sample i, as d_i. By taking the mean of distance measures surrounding $\vec{v}_i$ we get a smoother function d_i as compared to $d\,f_i$. This is due to the spreading of incidentally appearing high values of $d\,f_i$ caused by noisy artefacts. The concept can be generalized to arbitrary neighbourhoods of $\vec{v}_i$, taking more or less than 3 surrounding feature vectors into account. For the geoacoustic example experiments showed best results for d_i as presented above.

4.2 Problem Related Parameter Settings

Since the Gabor feature vector approach uses a lot of parameters it is hard to give some general statements on how to optimise all parameters for any given physical problem. We already mentioned two normalisations (center in time, normalise energy) in the previous paragraph. Here we discuss some other choices made for a specific physical problem, namely the geoacoustic propagation problem as described in Section 1. The choices we present here are based on experiments for different buoy tracks, i.e., tracks of the receiver in different regions of a shallow water environment. For more information on the setting and the tracks of the experiments we refer to [5].

The first choice to be made for this problem is whether all MP parameters should be weighted equally. After normalisation of all s_i in time, obviously we can omit the position parameters $t_{i,n}$. Experiments also validated this, as d_i was negligably effected by omitting $t_{i,n}$ in $\vec{v}_i$. Furthermore, experiments showed that the frequency parameters $f_{i,n}$ only had minor effect at d_i. Although d_i as a function of i was influenced by the omission of $f_{i,n}$, neither more or less characteristic changes in d_i appeared, according to local variations in the system (sea bottom parameters). Therefore, frequency parameters were not taken into account in the results in Section 5.

Concerning the remaining parameters, experiments showed that taking only the amplitude parameters $c_{i,n}$ into account most changes in the system are already reflected by the corresponding distance measures. However, experiments also showed that the scales $a_{i,n}$ yield a substantial contribution to the behaviour of d_i. In fact, some system changes not picked up by the amplitudes of the Gabor atoms only, were indicated by d_i after adding the amplitudes to the feature vectors $\vec{v}_i$. Resuming, for the geoacoustic example we will construct $2N$-dimensional feature vectors, given by

$$\vec{v}_i = (c_{i,1}, a_{i,1}, \cdots, c_{i,N}, a_{i,N}). \qquad (10)$$

The last parameter to pay attention to is the number of atoms N to be taken into account. Instead of experimenting with different numbers N, we vary the desired L^2 approximation error $\|s_i\|^2\cdot(1-E_{s_i}(N))$. This automatically yields the number N_i corresponding to that particular error. For the non-adaptive approach one can calculate one number of

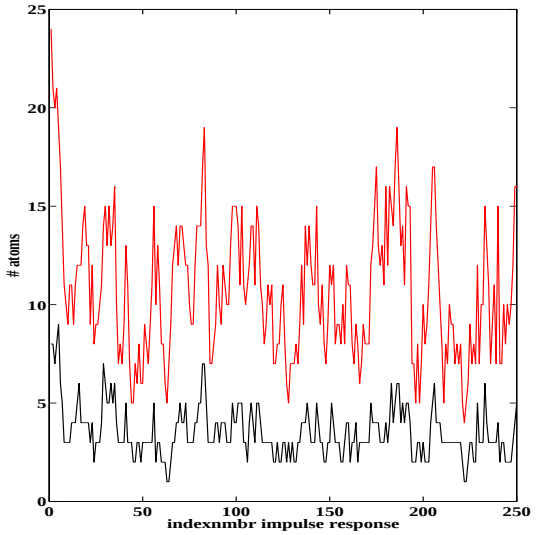

Figure 1: Number of atoms N_i corresponding to an energy ratio of 80% (black) and 90% (red) in the MP decomposition of 250 geoacoustic impulse responses.

atoms for all measured data. In Figure 1 we depicted N_i for 250 measured geoacoustic impulse response ($i = 1,\ldots,250$) for $E_{s_i} = 0.8$ (black) and $E_{s_i} = 0.9$ (red). Obviously, for the adaptive approach with $E_{s_i} = 0.9$ the dimension of the feature vectors (10) vary from 10 to 50, which emphasizes the difference between both methods. Furthermore, results obtained from measuring the vectors showed that $E_{s_i} > 0.9$ gave good results. Particularly, we took $E_{s_i} > 0.95$ for the results in the next Section.

5. A GEOACOUSTIC EXAMPLE

The geoacoustic example we discuss is taken from the so-called ENVERSE 97 experiments in a Mediterranean shallow water area by the NATO Undersea Research Center (NURC), see [5]. Acoustic impulse responses were measured on receiver buoys drifting away from a fixed source. Out of 8 different buoy tracks we have taken buoy track 1 for the example case, see Figure 2. The track of the buoy receiver (pink) is depicted for measurements taken between 14:00 and 17:30 hours on 3 November 1997. The buoy receiver crossed different types of sediment (blue/yellow) and sediment thickness (different color intensity). The geophysical survey ENVERSE 98 characterised the ocean bottom at particularly high spatial resolution using Swath multibeam system, Uniboom profiler and sediment cores. This characterisation of the bottom is used for GIS map in Figure 2. Finally, we observe that the 'proof of principle' for the Gabor feature vector approach was also using buoy 1, however only with modest success [2].

The geoacoustic impulse responses were obtained from 1 min repeated, long-duration chirp pulses with frequency band 0.8-1.6 kHz. Each of the impulse responses has been decomposed by teh Matching Pursuit algorithm and corresponding feature vectors have been constructed. For these vectors we used the normalisations, as described in Section 4. Due to these normalisations the ommission of the position and frequency parameters within the feature vectors is made possible. Comparing the adaptive and non–adaptive approach for $E_s(N) = 0.95$ showed a slightly better performance of the adaptive approach. For this amount of energy in the approximation a varying number of atoms N are used between 9 and 35, with an average of 18 atoms for all measurements (254).

Figure 3 shows the performance of our method for this particular example. The mean distances between feature vectors, as described in Section 4, has been depicted. Most of the major increases in distance measure are related to sediment changes, indicated by arrows and corresponding arrows in Figure 2. Only one sedimental change has not been picked up by our method. On the other hand also only two false alarms appear (14:20 and 15:25). The local maxima in Figure 3 bounded by red rectangular areas can be related to intrasedimental changes, that of course also change the physical conditions and therefore also the Green's functions measured at these positions. In Figure 2 these intrasedimental changes are indacted by closed white curves (with a blue background).

Finally, we observe that for this type of example the time-varying oceanography (sound speed profile) along the acoustic path may also produce artefacts. Moreover, the acoustic transmission path varies since the source location and successive receiving points are typically not collinear, the buoys being driven by the currents. Results, similar as shown here, were obtained for other buoy tracks from the ENVERSE experiments. For all other buoy tracks considered, the set–up and normalisations as discussed for the buoy 1 track gave also the best results for other tracks. Results for this and other tracks will be discussed in a forthcoming paper.

6. CONCLUSIONS

Gabor feature vectors have been proposed to analyse Green's functions of changing systems. Parameters within the proposed method have been discussed to find an optimal setting of the approach. Furthermore, to reduce the influence of noisy artefects an adaptive strategy has been introduced based on desired energy ratio levels for the approximation of Green's function by Gabor atoms.

A problem from underwater acoustics has been taken as an example of a system with changing Green's functions. We have shown that for this example a 1–1 relation between major changes at the sea bottom and changing Gabor feature vectors is established. Using this relation the unsupervised adaptive method demonstrated a good performance. Almost all bottom changes were correctly detected with only very few false alarms allowing to identify subareas of distinct geoacoustic properties.

Although the example discussed here showed good results for our method it cannot act like a model example allowing our method to perform similar on all similar problems. Moreover, some parameters in the method are optimised for this particular example. However, most considerations hold for a general setting, supporting the fact that the method can also be used for similar type of problems.

Acknowledgment

This research was carried out within the REA project at the Royal Netherlands Naval College and the joint project AO-BUOY with the NATO Undersea Research Centre (NURC), La Spezia, Italy. The ENVERSE 97-98 experimental data were provided by NURC. Special thanks to E. Michelozzi,

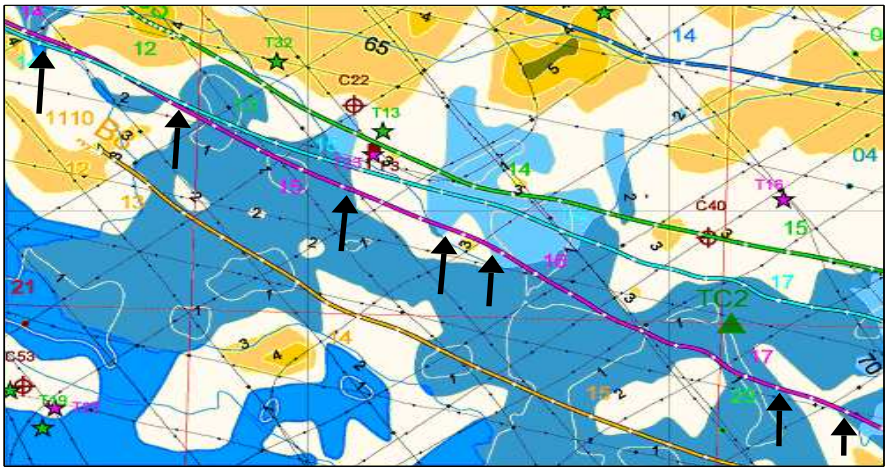

Figure 2: Track of buoy 1 (pink line) during the ENVERSE experiments, southern Marettimo (Sicily) shelf, 3 November 1997. The dots along the track are 10-min spaced time marks. The color map indicates the general nature of the bottom as determined from a geophysical survey in 1998. Modern sediments (yellow-brown) overly disconformably Pleistocene succession or fill pockets on a rough rocky substratum of Mesozoic limestones (blue). Adapted from Hermand et al. [5].

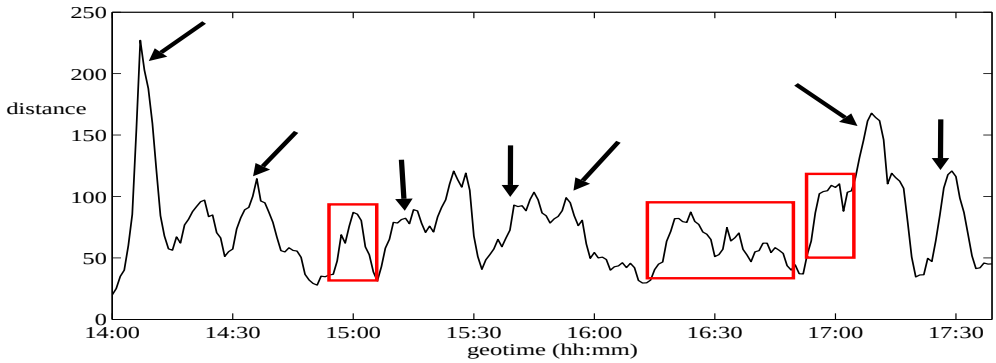

Figure 3: Averaged distances between consecutive Gabor feature vector. Most maximum values of the distances are related to sediment changes in Figure 2, indicated by corresponding arrows. Peaks within the red areas can be related to intrasedimental changes. Two major peaks can be considered as false alarms.

NURC, and M. Agate, Univ. of Palermo, for their involvement in the geophysical survey, and to P. Guerrini, P. Boni, F. Spina and P. Nardini, NURC, for the engineering support.

REFERENCES

[1] S. Mallat and Z. Zhang, "Matching pursuit with time-frequency dictionaries," *IEEE Trans. Sig. Proc.*, 41(12), 3397-3415, 1993.

[2] P.J. Oonincx and J.-P. Hermand,"Gabor Atomic Decomposition of Green's Functions for the Geoacoustic Inversion and Segmentation of Shallow Water Areas," *in Proc. IEEE Oceans Europe '05*, (CD-ROM), Brest, 2005.

[3] P.J. Huber, "Projection pursuit," *Ann. Stat.*, 13(2), 435-475, 1985.

[4] L.K. Jones, "On a conjecture of Huber concerning the convergence of projection pursuit regression," *Ann. Stat.*, 15(2), 880-882, 1987.

[5] J.-P. Hermand, P. Boni, E. Michelozzi, P. Guerrini, M. Agate, A. Borruso, A. D'Argenio, D. Di Maio, C. Lo Iacono, M. Mancuso, and M. Scannavino, "Geoacoustic inversion with drifting buoys: EnVerse1997-98 experiments," *in Proceedings of the Workshop on Experimental Acoustic Inversion Methods for Exploration of the Shallow Water Environment* (A.Caiti, J.-P. Hermand, S.Jesus, and M.B. Porter, eds.), Dordrecht, 263-286, Portuguese Foundation for Science and Technology, Kluwer Academic, June 2000.

[6] P.J. Oonincx and P.M. de Zeeuw, "Adaptive Lifting for Shape-Based Image Retrieval," *Pattern Recognition*, 36(11), 2663-2672, 2003.